Structural Monitoring and Maintenance, *Vol. 8, No. 3(2021) 221-234*
https://doi.org/10.12989/smm.2021.8.3.221

Effect of foundation uplift on seismic behavior of three-dimensional structure controlled with tuned mass damper

Hamid Mortezaie*[1] and Reza Zamanian [2]

[1] *Department of Civil Engineering, Faculty of Hamedan, Hamedan Branch, Technical and Vocational University (TVU), Hamedan, Iran*
[2] *Department of Earthquake Engineering, Tarbiat Modares University, nasr, jalal Al Ahmad St, 14115-111, Tehran, Iran*

(*Received May 27, 2019, Revised February 27, 2021, Accepted June 23, 2021*)

Abstract. In general, uplift causes changes in the structural system making its behavior and dynamic characteristics very different to common soil-structure models where no uplift is applied. Changes in rotational stiffness and lateral stiffness of structures, variations in radiation damping as well as the effective damping of structure are among the examples of these changes. Many valuable studies have been carried out in the past years about seismic control of structures with tuned mass damper (TMD) in case of two-dimensional shear structures with few performed in case of three-dimensional shear buildings. More realistic and complex models should be used in evaluating the seismic performance and design of controllers to simulate the actual behavior of buildings with higher accuracy. In this research, a three-dimensional finite element model has been created in OpenSees software with completely nonlinear and updated behavior of soil-structure system. The effects of uplift on soil-structure system equipped with TMD have been assessed using it. The conditions of employing TMD with variable stiffness have been evaluated with respect to the process carried out in this research. According to the results, based on the type of soil the structure has been designed based on, the uplift of structure can be reduced by installing TMD while it cannot be reliably used for reducing displacement and lateral acceleration of the structure. Finally, evaluation of other responses of the structure related to damages to the structure revealed the good performance of TMD.

Keywords: high-rise concrete structures; nonlinear analysis; soil-structure interaction; tuned mass damper; uplift

1. Introduction

Numerous and valuable studies on structures with passive seismic monitoring systems over the past four decades as well as the reflection of benefits of these type of systems being mainly the equipment cost and easy manufacturing process have prompted engineers to widely use them for reducing the loads applied to the structure caused by earthquake and wind (Spencer Jr and Nagarajaiah 2003, Liu *et al*. 2008). TMD is one of the simplest and most effective devices of passive control systems with low maintenance costs which increase the structural performance against environmental loads (Gerges and Vickery 2005, Shooshtari and Mortezaie 2017). This device includes a block with huge mass added to the structure which is either installed on the floor

*Corresponding author, Ph.D., E-mail: hamid.mortezaie@gmail.com

http://www.techno-press.org/?journal=smm&subpage=7 ISSN: 2288-6605 (Print), 2288-6613 (Online)

or hung from the ceiling similar to a pendulum. This mass is usually surrounded by several springs and viscous dampers in order to provide stiffness and damping. The public interest of engineering community to passive systems and especially TMD has led to more complementary studies to be carried out on understudied aspects of these systems.

Other than the type of the structure (concrete and steel structure, linear or nonlinear materials) (Fajfar 2000, Sgobba and Marano 2010, Aguirre and Almazán 2015, Shooshtari and Mortezaie 2017), type of structural analysis, algorithms and different methods of optimization for TMD parameters (Gerges and Vickery 2005, Bakre and Jangid 2007, Greco and Marano 2013, Aguirre and Almzán 2014) and consideration such as structural torsion (Singh *et al*. 2002, Li and Qu 2006, Tse *et al*. 2012), the issue which has attracted less attention in complementary studies is that TMD performance evaluation regardless of subsoil consideration is far from reality. Existence of soil under the foundation leads to lateral and rotational degrees of freedom in foundation and subsequently, the general behavior of soil-structure system changes (Jafarieh and Ghannad 2014). These changes in turn can increase or decrease the nonlinear behavior of structure, change the general behavior of soil-structure system and as a result change the system response which includes increasing lateral displacement and inter-story drift under earthquake load and eventually leads to corruption as well as loss of performance expected from the structure (Khatibinia *et al*. 2016, Khoshnoudian *et al*. 2016). That is why nowadays there is a severe need for simulating actual behavior of buildings with greater accuracy using more realistic and complex models to evaluate the performance of seismic control devices (Moehle *et al*. 2008, Nigdeli and Boduroğlu 2013).

There are a few studies about structures with TMD by considering the effect of soil-structure interaction where these few studies can be classified in two categories.

The first category is related to optimization of TMD parameters (Khatibinia *et al*. 2016, Bekdaş and Nigdeli 2017, Mortezaie and Rezaie 2018a) while the second is related to studies examining the effect of soil-structure interaction subjected to wind load (Liu *et al*. 2008, Farshidianfar and Soheili 2013) and earthquake load on structures with one floor (Ghosh and Basu 2004, Wang and Lin 2005) or several floors (Wu *et al*. 1999, Takewaki 2000). Khoshnoudian *et al*. (2017) evaluated three steel structures with a linear behavior and with TMD subjected to 52 near field earthquakes in order to evaluate the effects of soil-structure interaction. The results indicated that soil rupture reduces TMD efficiency.

Salvi *et al*. (2018) noted the importance of considering the effects of SSI. Their paper states that the efficiency rate of TMDs remains controversial and in addition, considering the SSI has a significant effect on the adjustment of TMDs.

In their study, Jia and Jianwen (2019) examined the effect of various parameters such as structure aspect ratios, height, the foundation embedment as well as the soil-layer thickness on the TMD performance. Also, they examined the structural responses by adjusting the TMDs in two modes of considering and neglecting the soil effects. They found that when the TMD is adjusted considering the effects of soil-structure interaction, their performance will be 25% better. On the other hand, this damper, in the case of adjustment while neglecting the effects of soil, reduced the response of the structure by 30%.

Abd-Elhamed and Mahmoud (2019) compared the response of structures considering the effects of SSI under near-field and far-field earthquakes. They showed that near-field records create a higher demand in the structure. Also, considering the effects of SSI would decrease the role of TMD in reducing the structural response.

Note that studies on soil-structure systems with TMDs have usually been carried out on two-dimensional shear structures by assuming linear behavior for materials.

In the present research, the simultaneous effects of soil-structure interaction (SSI), uplift of the foundation as well as inelastic behavior of the upper structure and subsoil have been evaluated with a detailed three-dimensional finite element model of a high-rise concrete structure designed using performance based plastic design (PBPD) equipped with TMD while considering the aspects already been mentioned. For this purpose, the time history analysis has been carried out on a twenty-story concrete structure model subjected to Kobe Shin Osaka and Northridge Beverly Hills earthquake records. Advanced Ibarra model (Haselton 2006) was used for modeling the concrete hysteresis behavior. Tuned Mass Spectra (Shooshtari and Mortezaie 2017, Mortezaie and Rezaie 2018b) has been used for optimizing the TMD parameters by evaluating the changes of seven criteria of structural responses.

In this research, we tried to investigate the performance of concrete structures equipped with TMDs by considering soil-structure interaction and level of structural damages.

2. Properties of evaluated high-rise concrete structure

A twenty-story concrete structure with a special moment frame system was designed based on instructions of PBPD method and further evaluated in this research.

The site of evaluated structure was Los Angeles, California with high seismic risk in accordance with ASCE7-10 (ASCE 2013) regulations with soil type of D. 28-day compressive strength of concrete in beams and columns was considered to be 35 MPa and 42 MPa respectively. The height of structural floors on the first floor and other floors were 460 cm and 400 cm respectively. The target design drift ratio was considered 2% and target yield drift 0.5%. The dead load of floors was equal to 850 kilograms per square meter and the live load of floors was considered 40 kilograms per square meter.

Tables 1-2 report the specifications and dimensions of beam and column elements along with three-dimensional tensile plus compressive reinforcements of the structure in two x and y directions. Fig. 1 displays the plan of structure and the plan of foundation along with dimensions and characteristics. It was assumed that the whole evaluated structure was placed on a shallow foundation at a depth of 3 meters from the ground.

3. Structural modeling

3.1 Specifications and model of soil

Calculation of seismic response of soil-foundation-structure system requires deep knowledge and understanding about basic parameters of soil such as dynamic stiffness of foundation, which is generally determined by coefficients of springs and dampers (Ghannad and Jafarieh 2014).

Non-linear time history analysis for the structure was carried out in this study for the same type of soil for which the structure was designed. The model presented in FEMA 440 (2005) (FEMA 2005) was used for this purpose to capture the SSI effect. A set of springs placed at the end of each column at the height equal to foundation was used for modeling the foundation and the foundation subsoil. This set of concentrated springs included a vertical spring in z direction with non-linear behavior, two horizontal transmission springs plus two rotational springs around x and y axes

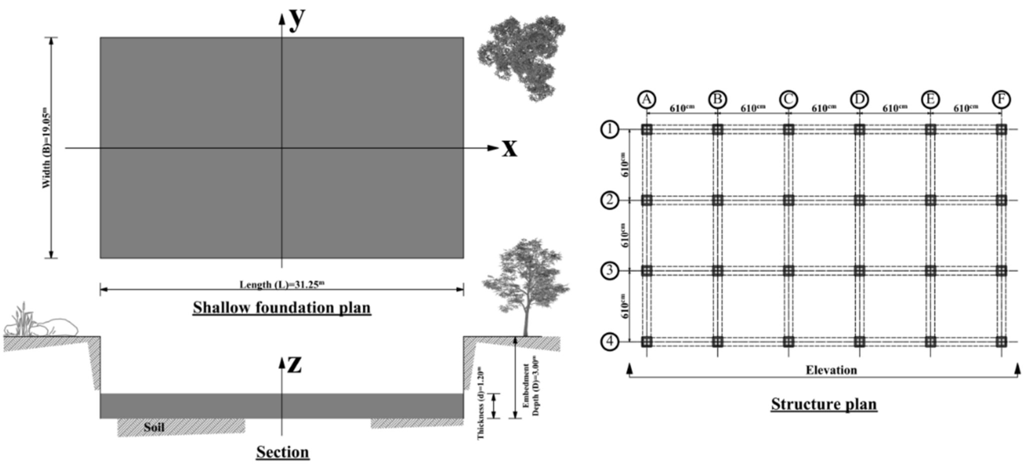

Fig. 1 Plan of structure and foundation along with a cross-section of foundation

Table 1 Specifications and dimensions of beam and column elements in two x and y directions

	Beams			Columns		
	size (cm)	ρ_{beam}[†] (%)	ρ'_{beam}[+] (%)	size (cm)	$\rho^*_{Exterior\ Column}$ (%)	$\rho^*_{Interior\ Column}$ (%)
Story 1	75×75	0.45	0.62	80×80	1.22	1.22
Story 2	75×75	0.39	0.62	80×80	1.49	1.98
Story 3	70×75	0.36	0.63	80×80	1.22	1.83
Story 4	70×75	0.35	0.62	80×80	1.22	1.49
Story 5	70×75	0.37	0.66	80×80	1.22	1.22
Story 6	65×70	0.41	0.75	75×75	2.26	2.77
Story 7	65×70	0.40	0.74	75×75	2.08	2.26
Story 8	65×70	0.39	0.72	75×75	2.08	2.08
Story 9	65×70	0.38	0.70	75×75	1.39	2.08
Story 10	65×70	0.36	0.69	75×75	1.13	2.08
Story 11	60×65	0.49	0.90	75×75	1.13	2.08
Story 12	60×65	0.48	0.86	75×75	1.13	2.08
Story 13	60×65	0.44	0.81	75×75	1.13	2.08
Story 14	60×65	0.38	0.76	70×70	1.59	2.39
Story 15	60×65	0.35	0.69	70×70	1.59	2.39
Story 16	40×55	0.54	1.10	70×70	1.59	2.39
Story 17	40×55	0.50	0.96	70×70	1.30	1.94
Story 18	40×55	0.44	0.79	70×70	1.30	1.94
Story 19	40×55	0.37	0.62	70×70	1.02	1.59
Story 20	40×55	0.35	0.35	70×70	1.02	1.02

[†]Tension Reinforcement ratio of beam; [+]Compression Reinforcement ratio of beam; [*]Reinforcement ratio of column

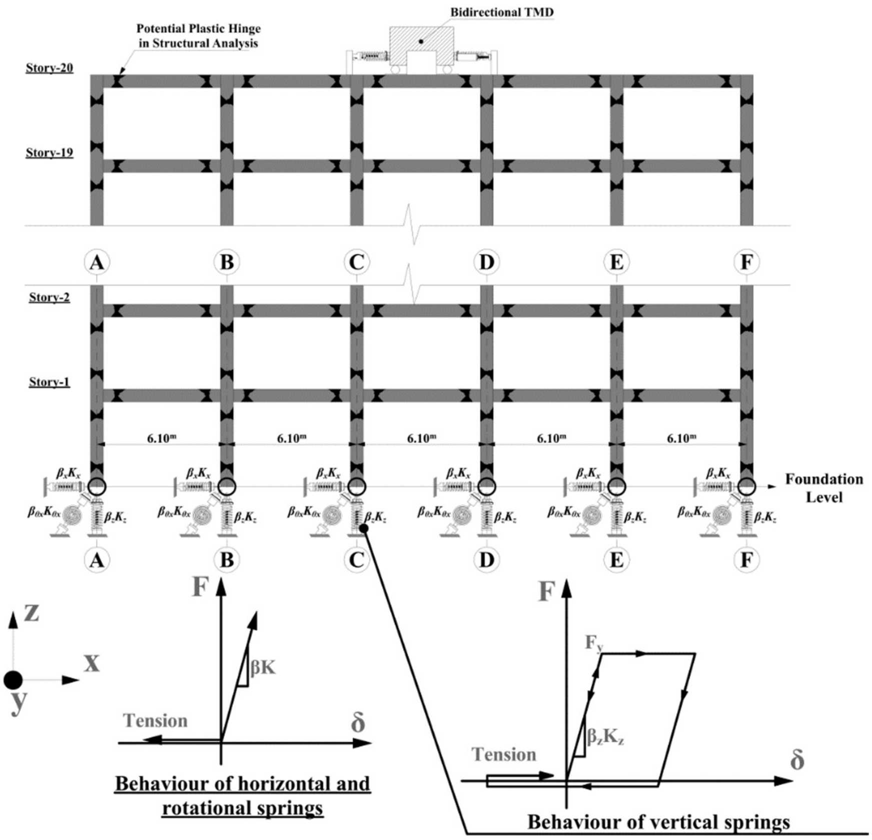

Fig. 2 Structural model in x direction

Table 2 Equations used for calculation of stiffness of springs and foundation depth coefficients (FEMA 2005)

Degree of freedom	Stiffness	Embedment factor
Horizontal translation (toward short side) x-direction	$K_x = \frac{GL}{2-\upsilon}\left(2+2.5\left(\frac{B}{L}\right)^{0.85}\right) - \frac{GL}{0.75-\upsilon}\left(0.1\left(1-\frac{B}{L}\right)\right)$	$\beta_x = \left(1+0.15\left(\frac{2D}{B}\right)^{0.5}\right) \times \left[1+0.52\left(16\frac{\left(D-\frac{d}{2}\right)(L+B)d}{LB^2}\right)^{0.4}\right]$
Horizontal translation (toward long side) y-direction	$K_y = \frac{GL}{2-\upsilon}\left(2+2.5\left(\frac{B}{L}\right)^{0.85}\right)$	$\beta_y = \left(1+0.15\left(\frac{2D}{B}\right)^{0.5}\right) \times \left[1+0.52\left(\frac{\left(D-\frac{d}{2}\right)16(L+B)}{L^2B}d\right)^{0.4}\right]$
Vertical translation z-direction	$K_z = \frac{GL}{1-\upsilon}\left(0.73+1.54\left(\frac{B}{L}\right)^{0.75}\right)$	$\beta_z = \left(1+0.095\frac{D}{B}\left(1+1.3\frac{B}{L}\right)\right) \times \left[1+0.2\left(\frac{(2L+2B)}{LB}d\right)^{0.67}\right]$

Table 2 Continued

Degree of freedom	Stiffness	Embedment factor
Rotation (about x axis)	$K_{\theta x} = \frac{GI_x^{0.75}}{1-\upsilon}\left(\frac{L}{B}\right)^{0.25}\left(2.4+0.5\frac{B}{L}\right)$	$\beta_{\theta x} = 1 + 2.52\left(\frac{d}{B}\right) \times \left(1 + \frac{2d}{B}\left(\frac{d}{D}\right)^{-0.20}\left(\frac{B}{L}\right)^{0.50}\right)$
Rotation (about y axis)	$K_{\theta y} = \frac{GI_y^{0.75}}{1-\upsilon}\left[3\left(\frac{L}{B}\right)^{0.15}\right]$	$\beta_{\theta y} = 1 + 0.92\left(\frac{2d}{L}\right)^{0.60} \times \left(1.5 + \left(\frac{2d}{L}\right)^{1.9}\left(\frac{d}{D}\right)^{-0.60}\right)$

Table 3 Specifications of type D soil, ultimate strength of soil and yield force of springs

Properties of the soil Class D						Yielding force for vertical springs	
$\bar{V}_s^{*}$ (m/s)	ν^{+}	$G_0^{\dagger}$ (kN/m²)	$G = 0.42G_0$☼ (kN/m²)	γ♠ (kN/m³)	$\bar{q}_{ult}^{\ddagger}$ (kN/m²)	Interior springs (kN)	Exterior springs (kN)
270	0.25	13700	5750	18.41	598.75	22100	16700

*Average shear wave velocity; +Poisson’s ratio; †Initial shear modulus; ☼Effective shear modulus; ♠Soil unit weight; ‡Average estimated value of ultimate bearing capacity

(Fig. 2).

The stiffness of these springs depends on mechanical characteristics of soil, foundation dimensions and depth of foundation from the ground according to equations presented in FEMA 440. Since the effect of soil conditions and characteristics of earthquake acceleration on nonlinear dynamic performance of structure have been evaluated in this research, the effects of radiation damping on the structural response have not been considered in this study.

It has been assumed that the only available damping is damping of materials in the structural system and this damping calculated using Rayleigh damping equation and dominant modes of structural system. Transitional stiffness of springs in x, y, and z directions are equal to $\beta_x K_x$ and $\beta_y K_y$ and $\beta_z K_z$ respectively which have been obtained based on equations presented in Table 2.

The specifications of soil with values mentioned in IBC 2000 (IBC 2000) have been considered in Table 3 through implementing the specifications mentioned for type D soil in ASCE regulation with IBC regulation. Springs used to model the soil and foundation system have been assumed to have compressive strength without tensile strength. In this research, the nonlinear behavior of soil was considered without any tensile strength for vertical springs according to Fig. 2 by assuming a bilinear simple deterioration model. The yield force of springs was obtained through multiplying the ultimate capacity of soil by effective surface of foundation. The equation presented in ATC-40 (1996) (Comartin *et al*. 2000) was used for estimating the ultimate capacity of soil

$$q_{ult} = (c \cdot N_c \cdot q_c) + (\gamma \cdot D \cdot N_q \cdot q_q) + \left(\frac{1}{2}\gamma \cdot B \cdot N_\gamma \cdot q_\gamma\right) \tag{1}$$

In this equation: c is the soil cohesion, N_c, N_q and N_y represent the bearing capacity factors of soil, q_c, q_q and q_y are factors of foundation shape. γ is the unit weight of soil volume, D is the depth of the buried foundations and B is the width of foundation. The final strength of the soil has been obtained based on soil profiles and Tables 7-10 of ATC-1996 regulation. In the end, the yield force of springs for external and internal supports was obtained according to Table 3. It has been assumed that horizontal and transverse springs will act in a linear elastic form without the ability to endure tension in accordance with Fig. 2.

3.2 Features of the structural model

The analysis and modeling of nonlinear structures based on incorrect and unrealistic methods can lead to incorrect and illogical answers. There are many finite element models for concrete structures. However, most of them are not able to simulate the structural failure.

Hysteresis model which has been used in this model for modelling the nonlinear behavior of reinforced concrete beam and column elements was calibrated and updated model of Ibarra as presented by Haselton (2006) and based on a series of extensive laboratory results. Haselton has presented a series of empirical equations based on the same experiments for parameters of this model for computational modelling. This model can capture important deterioration and strength reduction modes which can result in lateral collapse of the entire structure. Modelling was done in OpenSees software using beam-column element composed of an elastic element and two moment rotation hinges focused at both ends and with a length of zero (Fig. 3). The weight of each floor in the structure has been considered to be equal to other floors and equal to 4641 kN. This weight has been considered in the center of mass of each floor. The floor diaphragm of the structure has been assumed to be in form of rigid diaphragm.

Concerning the effect of earthquake in two directions perpendicular to each other, accidental eccentricity was considered 5% of the dimension of structure perpendicular to the earthquake only for earthquake in y direction for capturing the accidental torsion. First, the second and third oscillation frequencies of structure were 2.74 Hz, 3.17 Hz and 8.66 Hz respectively.

3.3 Applied base stimulations

Time history analysis was carried out on the introduced structural model using two far-field earthquake record accelerations for optimizing and evaluating TMD parameters. Each of these earthquakes has consisted of two earthquake records perpendicular to each other (in x and y directions). The acceleration recorded during Northridge and Kobe earthquakes along with

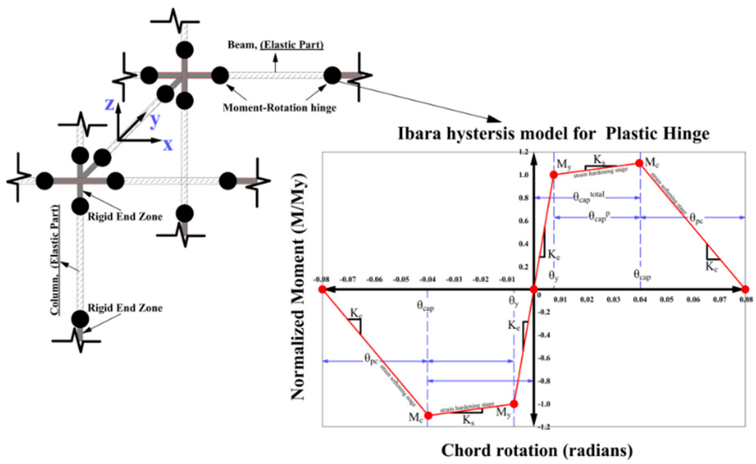

Fig. 3 Schematic image of beam and column element along with Ibara's hysteresis model

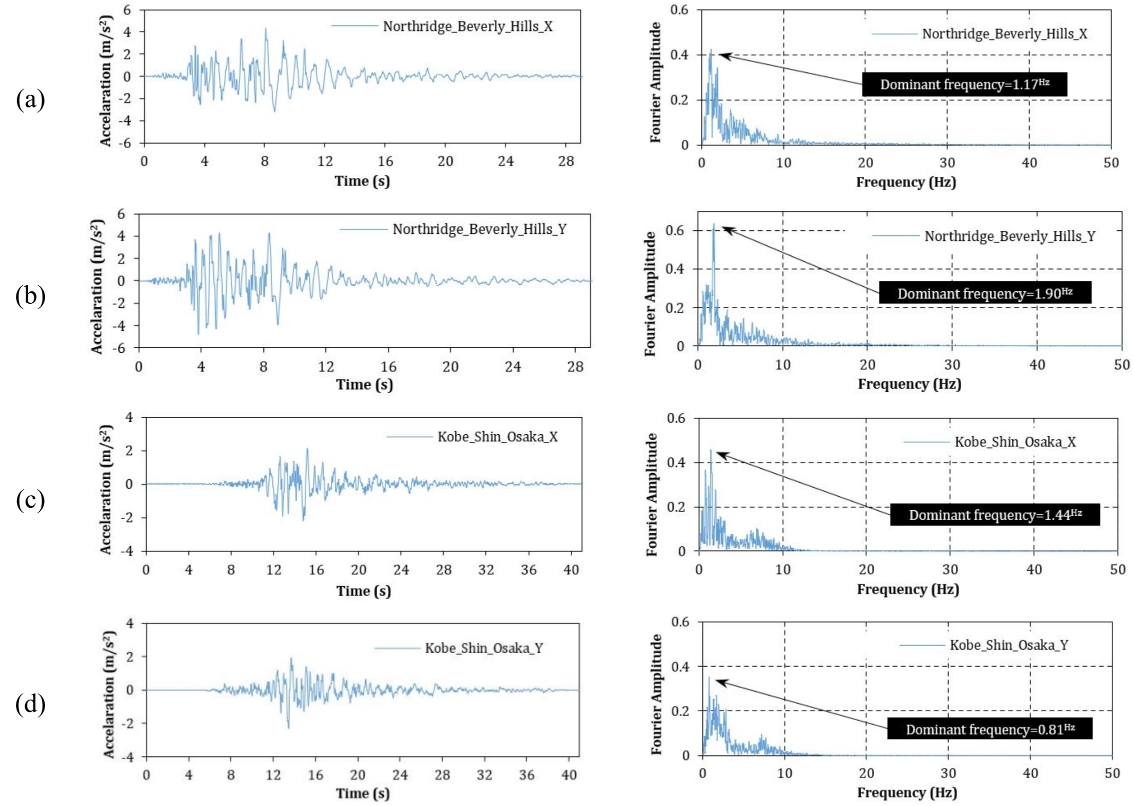

Fig. 4 Record of earthquake applied on two x and y directions along with Fourier series: (a) Northridge-Beverly hills-0°; (b) Northridge-Beverly hills-90°; (c) Kobe-Shin Osaka-0°; (d) Kobe-Shin Osaka-90°

Fourier series are shown in Fig. 4. As can be seen, the dominant frequencies of the Northridge earthquake in the directions of x and y are equal to 1.17 and 1.9 Hz, respectively, and the dominant frequencies of the Kobe earthquake in the directions of x and y are equal to 1.44 and 0.81 Hz, respectively. In addition, the Northridge earthquake has a narrower frequency band than the Kobe earthquake.

4. Evaluation of the results of the analyzing and optimizing TMD parameters

A TMD with three parameters of stiffness (K_d), damping (C_d) and mass (m_d) has been introduced whose optimization can increase the performance of TMD. The mass of TMD is generally considered as a percentage of total mass of the structure.

TMD damping can be achieved through multiplying the damping ratio by critical damping of TMD [$\xi_d = C_d/(2m_d \times \omega_d)$]. Also, as TMD adjusted for the structure, the tuning ratio (β) is the ratio of TMD vibration frequency to the structure vibration frequency ($\beta = \omega_d/\omega$).

The top performance of active mass damper (AMD) and semi-active mass damper (SAMD) has been different compared to TMD due to changes in stiffness of these controlling systems and increased versatility in those under different loads with frequency content.

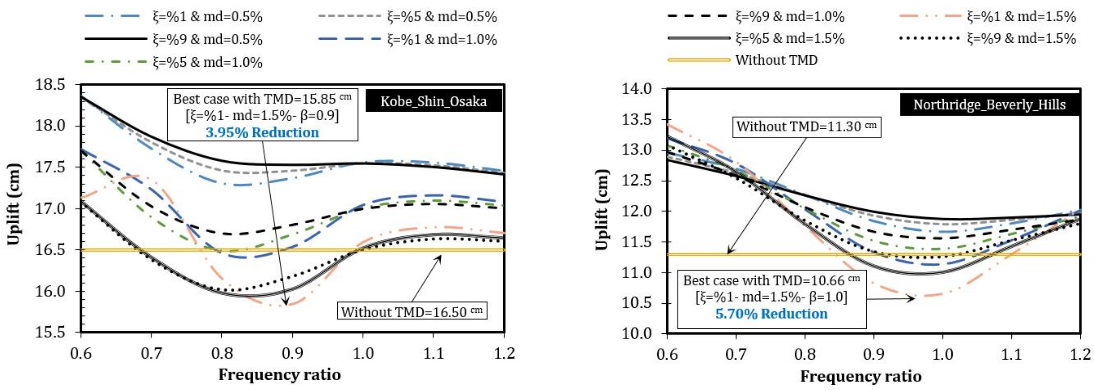

Fig. 5 Changes the maximum uplift occurred in the studied structure

Thus, β parameter which shows the TMD to structure stiffness ratio is clearly more important than mass and damping parameters of TMD. Thus, evaluation of changes in the maximum response of the structure under a range of different TMDs with different β coefficients can represent the performance of TMD and can be used in predicting AMD and SAMD performance.

Tuned mass spectra is a powerful method for evaluation of effects and optimization of TMD parameters in a certain earthquake (Shooshtari and Mortezaie 2017). In this study, the maximum response of the structure was obtained in each earthquake record using tuned mass spectra and based on performing 57 non-linear time history analysis on three-dimensional model of a twenty-story concrete structure with β changes from 0.6 to 1.2 for TMDs with different damping ratios of 1%, 5% and 9% as well as mass ratios of 0.5%, 1.0%, and 1.5%.

Fig. 5 reveals the uplift response of structure subjected to two Kobe and Northridge earthquakes respectively. As seen, TMD could reduce the maximum uplift up to 3.95% and 5.70% respectively. This level of reduction in each earthquake occurred within different ranges of β coefficient.

Also, at a specified mass ratio with changing the TMD damping, no particular changes could be observed in the uplift of structure. The improvement in TMD performance in reduction of occurred uplift in the structure was clearly evident upon increasing the mass of TMD.

The structure was analyzed in the same soil type, which was designed for it. As seen in Fig. 5, the maximum uplift in the structure has not been negligible. This level of uplift certainly affects other structural responses. Since evaluation of one parameter cannot lead to achieving a proper judgment about the performance of the studied structure, other responses such as displacement, inter-story drift, dissipated plastic energy, base shear force and acceleration, as well as number of plastic hinges in structure subjected to these two earthquakes have been evaluated (Fig. 6). As seen in most presented diagrams, changing damping has not greatly affected the structure, and increased mass generally improved the performance of TMD.

TMD reveals a poor performance in controlling the maximum lateral displacement in Kobe earthquake unlike Northridge.

In the case of Kobe earthquake, only if m_d, ξ and β are 1.5%, 9% and 0.7, respectively, the maximum displacement will be reduced by 0.11%, and in other ratios under this earthquake, there will be an increase in maximum lateral displacement of the structure, which the maximum increasing is 4.76%. While in the Northridge earthquake in the β values about 0.6 to 0.8,

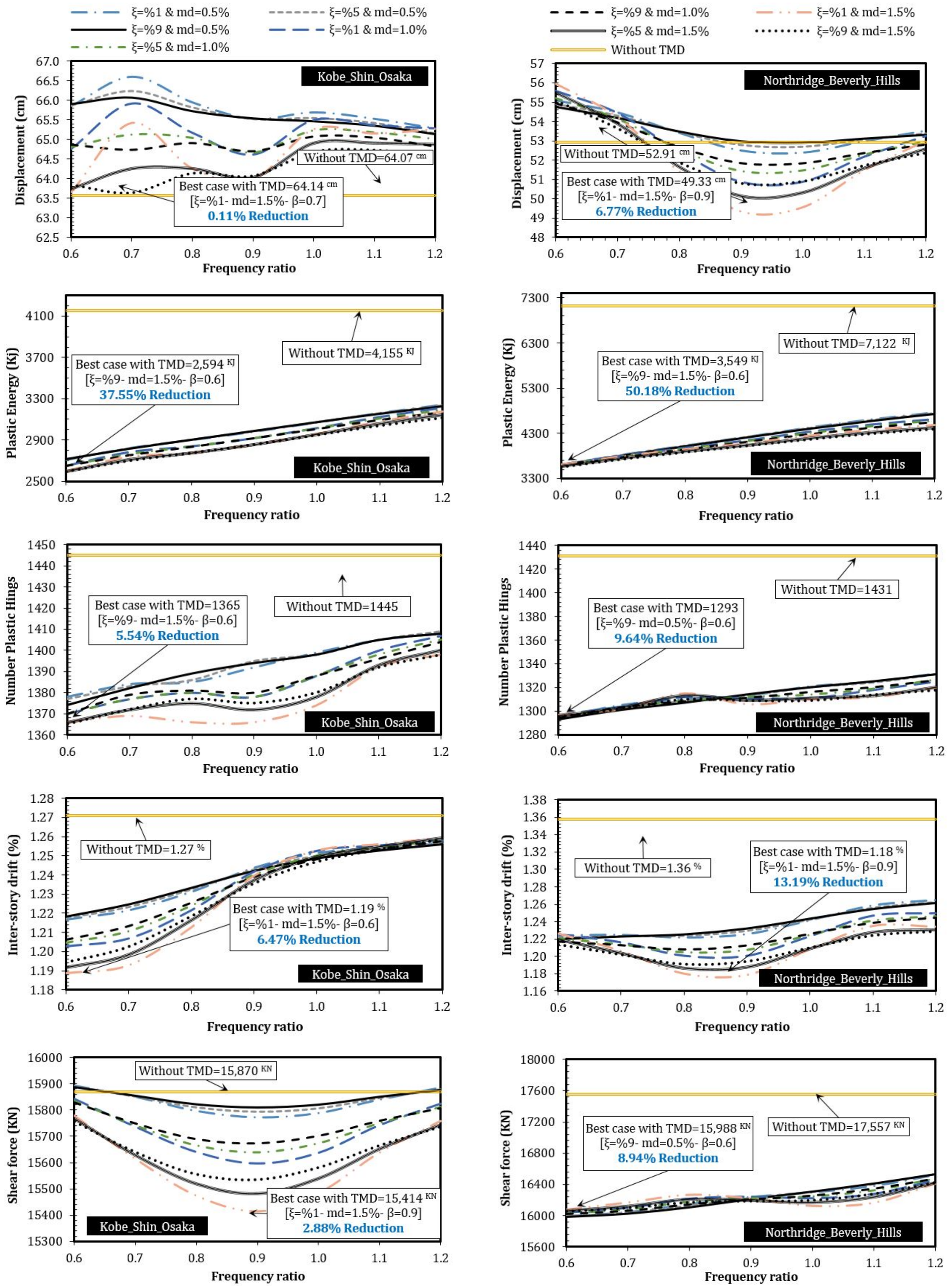

Fig. 6 Range of changes of other responses of structure subjected to two earthquake records

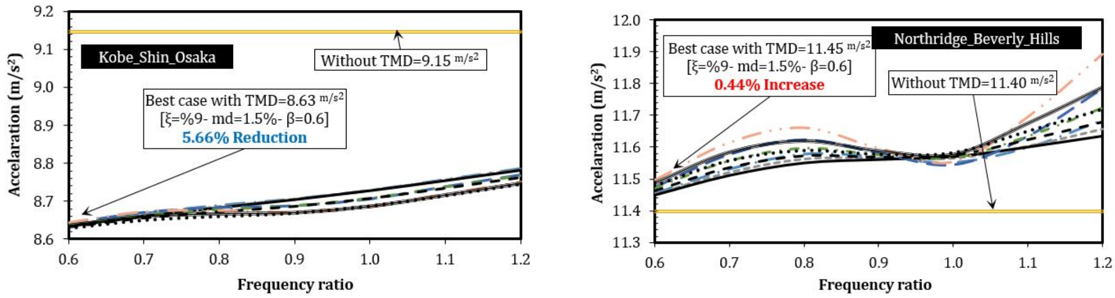

Fig. 6 Continued

increasing in displacement and in the intermediate β values, decreasing in maximum lateral displacement to 6.77% can be observed.

The performance of TMD in controlling the maximum plastic energy and the total number of plastic hinges of structures is very favorable. The reduction in plastic energy in the Kobe and Northridge earthquakes is at best 37.55% and 50.18%, respectively, which does not depend on the m_d and ξ, and is seen in β equal to 0.6. Changes of wasted plastic energy shows a linear behavior compared to β coefficient in a way that increased β coefficient reduces the optimal performance of TMD. Since reduced maximum plastic energy used in the structure lowers the total number of formed plastic hinges, it can be concluded that TMD reduces damages to the structure as well as the number of damaged areas. TMD mass has a minor effect on reducing plastic energy wasted in the structure.

In the inter-story drift diagram, reduction of β coefficient improves the performance of TMD subjected to Kobe earthquake. A decrease in inter-story drift between 1% and 6.47% can be seen in the diagram. Meanwhile, we observe the optimal performance of TMD in Northridge earthquake in the central ranges of β coefficient. The decrease in drift is 13.19% at best and 7.14% at worst.

Equipping the structure with TMD would reduce the base shear force which is greater in case of Northridge earthquake, which is about 8% to 9%. This reduction in the Kobe earthquake reaches a maximum of 2.88%. Since lower acceleration of the structure during earthquake reduces loss of life resulting from elements connected to the structure, its evaluation is vital. Evaluation of the structural acceleration in the last evaluated diagram did not show the same behavioral pattern in the two evaluated earthquakes; TMD led to increased acceleration in all evaluated ranges in Northridge earthquake from 0.44% to 4.3%, while it showed a different behavior in Kobe earthquake which would reduce the acceleration from 4.26% to 5.66%.

Figs. 5-6 suggest that TMD can be used for reducing uplift, wasted plastic energy, number of formed plastic hinges, base shear force, and inter-story drift; however, the optimum parameters of TMD are different in each one of responses as shown in the presented diagrams. Since damping has a slight effect on the evaluated response, use of a TMD with variable stiffness can overcome this problem. Thus, usage of TMD with variable stiffness is recommended. The desirable range of stiffness changes (β coefficient) subjected to evaluated earthquakes is 0.7-1.05. TMD does not show a reliable behavior in controlling acceleration and displacement of structure.

5. Conclusions

In this research, considering the effect of soil and consequently the effect of uplift on a completely nonlinear soil-structure system, a comprehensive evaluation of responses affecting the efficiency and performance of the structure was performed. The results of three-dimensional analysis of twenty-story concrete structures were provided under the effect of two far-field earthquake records with a range of TMDs with different parameters. The results indicated that although the effects of TMD on reducing the displacement response and structure acceleration are unreliable, but TMD showed a good performance in reducing the damage to the structure. In the case of Kobe earthquake, if β is equal to 0.7, the maximum displacement will be reduced by 0.11%, and in other ratios, there will be an increase in maximum lateral displacement of the structure, which the maximum increasing is 4.76%. In the Northridge earthquake, a reduction in displacement occurs in the intermediate β values, and this reduction is 6.77%. TMD led to increased acceleration in all evaluated ranges in Northridge earthquake from 0.44% to 4.3%, while it showed a different behavior in Kobe earthquake which would reduce the acceleration from 4.26% to 5.66%. The reduction in plastic energy in the Kobe and Northridge earthquakes is at best 37.55% and 50.18%. Engineers are recommended to consider use of TMD in the structure in structural design phase. Also, the use of TMD with variable stiffness instead of using TMD with constant stiffness is recommended as much as possible for providing the optimal performance for a structure.

References

Abd-Elhamed, A. and Mahmoud, S. (2019), "Simulation analysis of TMD controlled building subjected to far-and near-fault records considering soil-structure interaction", *J. Build. Eng.*, **26**, 100930. https://doi.org/10.1016/j.jobe.2019.100930

Aguirre, J. and Almzán, J. (2014), "Optimum seismic design of nonlinear asymmetric structures controlled by large tuned mass dampers", *Proceedings of the 10th US National Conference on Earthquake Engineering Frontiers of Earthquake Engineering*, anchorage, AL, USA, July.

Aguirre, J.J. and Almazán, J.L. (2015), "Damage potential reduction of optimally passive-controlled nonlinear structures", *Eng. Struct.*, **89**, 130-146. https://doi.org/10.1016/j.engstruct.2015.01.009

ASCE (2013), Minimum design loads for buildings and other structures, Amer Society of Civil Engineers. https://doi.org/10.1061/9780784412916

Bakre, S.V. and Jangid, R.S. (2007), "Optimum parameters of tuned mass damper for damped main system", *Struct. Control Health Monitor.*, **14**(3), 448-470. https://doi.org/10.1002/stc.166

Bekdaş, G. and Nigdeli, S.M. (2017), "Metaheuristic based optimization of tuned mass dampers under earthquake excitation by considering soil-structure interaction", *Soil Dyn. Earthq. Eng.*, **92**, 443-461. https://doi.org/10.1016/j.soildyn.2016.10.019

Comartin, C.D., Niewiarowski, R.W., Freeman, S.A. and Turner, F.M. (2000), "Seismic evaluation and retrofit of concrete buildings: a practical overview of the *ATC 40* Document", *Earthq. Spectra*, **16**(1), 241-261. https://doi.org/10.1193/1.1586093

Fajfar, P. (2000), "A nonlinear analysis method for performance-based seismic design", *Earthq. spectra*, **16**(3), 573-592. https://doi.org/10.1193/1.1586128

Farshidianfar, A. and Soheili, S. (2013), "Ant colony optimization of tuned mass dampers for earthquake oscillations of high-rise structures including soil–structure interaction", *Soil Dyn. Earthq. Eng.*, **51**, 14-22. https://doi.org/10.1016/j.soildyn.2013.04.002

FEMA, A. (2005), "440, Improvement of nonlinear static seismic analysis procedures", FEMA-440, Redwood City.

Gerges, R.R. and Vickery, B.J. (2005), "Optimum design of pendulum-type tuned mass dampers", *Struct. Des. Tall Special Build.*, **14**(4), 353-368. https://doi.org/10.1002/tal.273

Ghannad, M.A. and Jafarieh, A.H. (2014), "Inelastic displacement ratios for soil–structure systems allowed to uplift", *Earthq. Eng. Struct. Dyn.*, **43**(9), 1401-1421. https://doi.org/10.1002/eqe.2405

Ghosh, A. and Basu, B. (2004), "Effect of soil interaction on the performance of tuned mass dampers for seismic applications", *J. Sound Vib.*, **274**(3), 1079-1090. https://doi.org/10.1016/j.jsv.2003.09.060

Greco, R. and Marano, G.C. (2013), "Optimum design of tuned mass dampers by displacement and energy perspectives", *Soil Dyn. Earthq. Eng.*, **49**, 243-253. https://doi.org/10.1016/j.soildyn.2013.02.013

Haselton, C.B. (2006), "Assessing seismic collapse safety of modern reinforced concrete moment frame buildings", Doctoral Dissertation; Stanford University.

IBC (2000), International building code, International Code Council: Falls Church.

Jafarieh, A.H. and Ghannad, M.A. (2014), "The effect of foundation uplift on elastic response of soil-structure systems", *Int. J. Civil Eng.*, **12**(2), 146-157.

Jia, F. and Jianwen, L. (2019), "Performance degradation of tuned-mass-dampers arising from ignoring soil-structure interaction effects", *Soil Dyn. Earthq. Eng.*, **125**, 105701. https://doi.org/10.1016/j.soildyn.2019.05.040

Khatibinia, M., Gholami, H. and Labbafi, S. (2016), "Multi–objective optimization of tuned mass dampers considering soil–structure interaction", *Int. J. Optim. Civil Eng.*, **6**(4), 595-610.

Khoshnoudian, F., Ziaei, R. and Ayyobi, P. (2017), "Effects of nonlinear soil–structure interaction on the seismic response of structure-TMD systems subjected to near-field earthquakes", *Bull. Earthq. Eng.*, **15**(1), 199-226. https://doi.org/10.1007/s10518-016-9963-y

Li, C. and Qu, W. (2006), "Optimum properties of multiple tuned mass dampers for reduction of translational and torsional response of structures subject to ground acceleration", *Eng. Struct.*, **28**(4), 472-494. https://doi.org/10.1016/j.engstruct.2005.09.003

Liu, M.-Y., Chiang, W.-L., Hwang, J.-H. and Chu, C.-R. (2008), "Wind-induced vibration of high-rise building with tuned mass damper including soil–structure interaction", *J. Wind Eng. Indust. Aerodyn.*, **96**(6), 1092-1102. https://doi.org/10.1016/j.jweia.2007.06.034

Moehle, J.P., Hooper, J.D. and Lubke, C.D. (2008), "Seismic design of reinforced concrete special moment frames: a guide for practicing engineers", In: *NEHRP Seismic Design Technical Brief No. 1*, National Institute of Standards and Technology, U.S. Department of Commerce.

Mortezaie, H. and Rezaie, F. (2018a), "Effect of soil in controlling the seismic response of three-dimensional PBPD high-rise concrete structures", *Struct. Eng. Mech., Int. J.*, **66**(2), 217-227. https://doi.org/10.12989/sem.2018.66.2.217

Mortezaie, H. and Rezaie, F. (2018b), "Optimization and evaluation of three-dimensional high-rise concrete structure equipped by TMD with considering the soil-structure interaction effect", *J. Vibroeng.*, **20**(5), 2099-2110. https://doi.org/10.21595/jve.2017.18628

Nigdeli, S.M. and Boduroğlu, M.H. (2013), "Active tendon control of torsionally irregular structures under near-fault ground motion excitation", *Comput.-Aided Civil Infrastr. Eng.*, **28**(9), 718-736. https://doi.org/10.1111/mice.12046

Salvi, J., Pioldi, F. and Rizzi, E. (2018), "Optimum tuned mass dampers under seismic soil-structure interaction", *Soil Dyn. Earthq. Eng.*, **114**, 576-597. https://doi.org/10.1016/j.soildyn.2018.07.014

Sgobba, S. and Marano, G.C. (2010), "Optimum design of linear tuned mass dampers for structures with nonlinear behaviour", *Mech. Syst. Signal Process.*, **24**(6), 1739-1755. https://doi.org/10.1016/j.ymssp.2010.01.009

Shooshtari, M. and Mortezaie, H. (2017), "Effect of using linear multiple tuned mass dampers on concrete structures with hysteresis behavior", *J. Vibroeng.*, **19**(2), 1158-1172. https://doi.org/10.21595/jve.2016.17487

Singh, M.P., Singh, S. and Moreschi, L.M. (2002), "Tuned mass dampers for response control of torsional buildings", *Earthq. Eng. Struct. Dyn.*, **31**(4), 749-769. https://doi.org/10.1002/eqe.119

Spencer Jr, B. and Nagarajaiah, S. (2003), “State of the art of structural control”, *J. Struct. Eng.*, **129**(7), 845-856. https://doi.org/10.1061/(ASCE)0733-9445(2003)129:7(845)

Takewaki, I. (2000), “Soil–structure random response reduction via TMD-VD simultaneous use”, *Comput. Methods Appl. Mech. Eng.*, **190**(5), 677-690. https://doi.org/10.1016/S0045-7825(99)00434-X

Tse, K., Kwok, K. and Tamura, Y. (2012), “Performance and cost evaluation of a smart tuned mass damper for suppressing wind-induced lateral-torsional motion of tall structures”, *J. Struct. Eng.*, **138**(4), 514-525. https://doi.org/10.1061/(ASCE)ST.1943-541X.0000486

Wang, J.-F. and Lin, C.-C. (2005), “Seismic performance of multiple tuned mass dampers for soil–irregular building interaction systems”, *Int. J. Solids Struct.*, **42**(20), 5536-5554. https://doi.org/10.1016/j.ijsolstr.2005.02.042

Wu, J., Chen, G. and Lou, M. (1999), “Seismic effectiveness of tuned mass dampers considering soil–structure interaction”, *Earthq. Eng. Struct. Dyn.*, **28**(11), 1219-1233. https://doi.org/10.1002/(SICI)1096-9845(199911)28:11<1219::AID-EQE861>3.0.CO;2-G

JK